Molecular Mechanics in Crystalline Media: The Case of (*E*)-Stilbenes

Simona Galli, Pierluigi Mercandelli, and Angelo Sironi*

Contribution from the Dipartimento di Chimica Strutturale e Stereochimica Inorganica e Centro CNR CSSMTBO, via Venezian 21, I-20133 Milano, Italy

Received December 9, 1998. Revised Manuscript Received February 18, 1999

Abstract: Molecular mechanics simulations within the field of the *mean* (when disorder is present) crystal lattice have been used to settle most of the ambiguities inherent to the interpretation of the diffraction experiments on (*E*)-stilbenes. A dynamic process can be inferred by diffraction methods only if it leaves a track in the atomic displacement parameters or gives rise to some disorder or to some anomaly in the bonding parameters. However, since diffraction experiments map (according to Boltzmann's statistics) only the bottom of the local minima of the potential energy surface, many possible sources of misunderstanding are present. Indeed, the coupling of molecular mechanics to Kitaigorodsky's atom−atom pairwise potential approach, offering a detailed description of the solid-state trajectories (and of the involved energy changes) of (*E*)-stilbenes, has allowed a rationalization of the observed dynamic molecular disorder, which differently affects different crystal sites, and has led to a *quantitative* description of the anomalous temperature dependence of the ethylene bonding parameters in these compounds.

Introduction

We have recently devised a general, computationally easy method, which couples molecular mechanics (MM) to Kitaigorodsky's atom−atom pairwise potential (AAPP), to minimize the steric energy of a molecule, polymer, surface, or net within the field of a fixed, or periodically updated, crystal lattice.[1] These MMAAPP computations afford the "solid state" conformation of the molecule, its intramolecular steric energy, and its interaction energy with the surrounding lattice and are ideally suited for studying relative stabilities of different polymorphs, plastic deformations of a whole crystal lattice, molecular motions of flexible guest molecules in host crystal lattices, and factors controlling solid-state reactivity. In this paper we will show that our approach helps in understanding the solid-state dynamics of a class of *flexible* molecules, namely (*E*)-stilbenes, by offering a detailed description of their solid-state trajectories (and of the involved energy changes), allows a rationalization of the observed dynamic molecular disorder which differently affects different crystal sites, and leads to a *quantitative* description of the anomalous temperature dependence of the ethylene bonding parameters in these compounds.

The crystal structure of (*E*)-stilbene (**1**) was first determined, as early as 1937, by Robertson and Woodward[2] using photographic methods, but owing to the peculiarities of X-ray diffraction results and the relevance of **1** to many theoretical and spectroscopic investigations, it has been subsequently redetermined many times in different experimental conditions.[3−6] **1** crystallizes in the monoclinic system, space group $P2_1/c$, with two half independent molecules in the asymmetric unit, $\mathbf{1}_\alpha$ and $\mathbf{1}_\beta$, both lying about inversion centers (the 2*b* and 2*c* Wyckoff positions, hereafter labeled as α and β sites, respectively) and both nearly planar. Some orientational disorder affects the α site (actually occupied by molecules in two different orientations, $\mathbf{1}_\alpha$ and $\mathbf{1}_{\alpha'}$, almost related by a 180° rotation about the C(1)···C(1′) axis) but not the β one (Figure 1).

At room temperature (hereafter rt), the two independent ethylene bonds, C(7)−C(7′) of $\mathbf{1}_\alpha$ and $\mathbf{1}_\beta$ are apparently shorter (0.05 and 0.02 Å, respectively) than the standard length of an isolated ethylene bond (1.337 Å), and on lowering the temperature, their length increases (at 113 K, the bond in $\mathbf{1}_\alpha$ is still shorter than expected, while that in $\mathbf{1}_\beta$ approaches the "normal" value). It is noteworthy that no other bond in **1** displays a similar behavior, much smaller lengthening effects being observed on decreasing the temperature. In addition, all angles but those involving the C(7)−C(7′) bond have quite normal values and are just marginally dependent on temperature. In detail, the C(1)−C(7)−C(7′) bond angles and the C(6)−C(1)−C(7)−C(7′) dihedral angles substantially differ from the predicted values and significantly change, decreasing or increasing, respectively, as the temperature is lowered (see Table 1).

The temperature dependence shown by the quoted bonding parameters casts some doubts on the quality of their estimates, which should not be regarded as real but, rather, as an artifact due to some local dynamic process taking place in the crystal. Since the anomalous shrinking of the ethylene bond *without orientational disorder*[7] has been observed, at rt, in many compounds having the (*E*)-stilbene skeleton, such as (*E*)-2,2′-dimethylstilbene (**2**) (Scheme 1), Ogawa and co-workers[8] (hereafter Ogawa) decided to study **2** in order to understand the β-site behavior. On performing diffraction experiments on **2** at four different temperatures (118, 175, 234, and 298 K), he

(1) Mercandelli, P.; Moret, M.; Sironi, A. *Inorg. Chem.* **1998**, *37*, 2563−2569.

(2) Robertson, J. M.; Woodward, I. *Proc. R. Soc. London, Ser. A* **1937**, *162*, 568−583.

(3) Finder, C. J.; Newton, M. G.; Allinger, N. L. *Acta Crystallogr.* **1974**, *B31*, 411−415.

(4) Bernstein, J. *Acta Crystallogr.* **1975**, *B31*, 1268−1271.

(5) Hoekstra, H. A.; Meertens, P.; Vos, A. *Acta Crystallogr.* **1975**, *B31*, 2813−2817.

(6) Boustra, J. A.; Schouten, A.; Kroon, J. *Acta Crystallogr.* **1984**, *C40*, 428−431.

(7) Tirano-Rives, J.; Fronczek, F. R.; Gandour, R. D. *Acta Crystallogr.* **1985**, *C41*, 1327−1329. Ogawa, K.; Suzuki, H.; Sakurai, T.; Kobayashi, K.; Kira, A.; Toriumi, K. *Acta Crystallogr.* **1988**, *C44*, 505−508.

(8) Ogawa, K.; Takashi, S.; Yoshimura, S.; Takeuchi, Y.; Toriumi, K. *J. Am. Chem. Soc.* **1992**, *114*, 1041−1051.

10.1021/ja9842417 CCC: $18.00
Published on Web 04/03/1999

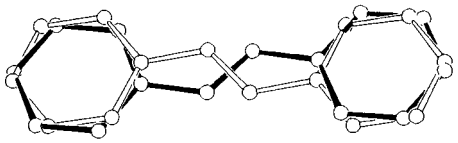

Figure 1. Superimposition of the two disordered individuals at the α site of (*E*)-stilbene (**1**$_\alpha$ + **1**$_{\alpha'}$). The two molecules are almost related by a 2-fold rotation about the C(1)···C(1′) axis.

discovered that, as the temperature is lowered, the C(7)−C(7′) bond length significantly increases, although remaining shorter than in an isolated C═C double bond. He also found that the C(1)−C(7)−C(7′) and C(6)−C(1)−C(7)−C(7′) angles show a marked temperature dependence, as in **1**, reaching (almost) reliable values only at 118 K, whereas all other bonding parameters are substantially temperature insensitive. Accordingly, since a rigid body libration of the whole molecule could not account for the above behavior, Ogawa suggested that *moderate* vibrations of the C(6)−C(1)−C(7)−C(7′) and C(7)−C(7′)−C(1′)−C(6′) dihedral angles may promote the interconversion, through a flat transition state, of two enantiomeric forms, which are related by a reflection plane almost parallel to the aromatic rings and differ in the orientation of the ethylene bond. At this point, the supposed presence of two enantiomers led Ogawa to reconsider the orientational disorder problem and discover that it affected also **2** (see Figure 2). As expected for a dynamic process, the disorder ratio was temperature-dependent, ranging from 0.65:0.35 at 298 K to 0.90:0.10 at 118 K, and this dependence allowed the computation of the enthalpy difference between the two enantiomeric forms in their crystalline environment. Differently, in **1**$_\beta$, Ogawa was unable to separate the contribution of two enantiomers but suggested their hidden presence in order to describe the dynamics occurring at this site and explain the temperature dependence of ethylene bond length.

Eventually, dealing with (*E*)-azobenzene, which is isomorphous to (*E*)-stilbene, Ogawa[9] suggested that the very same dynamic process he proposed for **1**$_\beta$ and **2** was also operative in **1**$_\alpha$, but due to the different crystalline environment, *its amplitude was somewhat larger*. Indeed, large vibrations of the C(6)−C(1)−C(7)−C(7′) and C(7)−C(7′)−C(1′)−C(6′) torsional angles may lead to a transition state with the ethylene bond almost orthogonal to the plane of the aromatic rings and eventually result in a 180° rotation of the ethylene bond about the C(1)···C(1′) axis (see Figure 3).

Following these observations, we developed an interest in (i) explaining the disorder at the α site and the short ethylene bond at the β one in compound **1**, through a molecular mechanics and a thermodynamic approach; (ii) testing Ogawa dynamic models for **1**$_\alpha$, **1**$_\beta$, and **2** with the aid of molecular mechanics computations; (iii) calculating the mean values of selected temperature-dependent geometrical parameters of **1**$_\beta$ and of **2**, applying Boltzmann's statistics to the molecular mechanics results.

Methodology

Molecular Mechanics Calculations. All of the computations have been done employing a local version of MM3 upgraded in order to deal with crystal lattices. Minimizations were carried out with the full-matrix Newton−Raphson algorithm using the standard MM3(92) force field[10] and employing a delocalized description of the conjugated π-system. Initially, for each phase, the experimental molecular conformation was allowed to relax in a periodically updated crystal lattice, with cell parameters fixed to their rt experimental values, to reach the closest minimum of the potential energy surface. Then, the whole crystal structure was minimized, optimizing alternatively the cell parameters and the conformation of the independent molecules. For species **1**, the experimental parameters were in fair agreement with their optimized values (a = 15.705 (15.674) Å, b = 5.725 (5.729) Å, c = 12.379 (12.298) Å, β = 111.895 (111.730)°, V = 1032.7 (1025.8) Å^3), so that the former set could be adopted in all of the following calculations. On the contrary, a comparison between the experimental and the optimized parameters for **2** (a = 10.892 (10.852) Å, b = 6.695 (7.205) Å, c = 8.681 (7.920) Å, β = 98.540 (94.277)°, V = 626.0 (617.6) Å^3) revealed some discrepancy, and both were employed in subsequent computations to check the consistency of the results.

Finally, all simulations of the solid-state dynamics were performed in a fixed crystalline environment, driving the selected molecule along the desired reaction coordinate.

Disordered Systems. To model disordered crystals, we allow the presence of "fractions" of a molecule in our computations. In ref 1 we defined our model of the crystal as constituted by the ensemble of a "reference molecule" (RM), and a set of "surrounding molecules" (SM), generated applying the appropriate space group symmetry operations to the RM. The latter could indeed contain more than one independent molecule, but no explicit reference to this point was originally made. At variance, in the following we briefly develop the formalism for dealing with more than one molecule *per* RM.

As for the simple case of a single independent molecule, the steric energy *per* RM *cluster* in the crystal (E_s) is still partitioned as follows:

$$E_s = E_{intra} + E_{inter}$$

E_{intra} is the sum of the conventional (*intra*molecular) steric energies for the n individual molecules constituting the RM, each weighted by its site occupancy factor (w_i, i = 1, ..., n)

$$E_{intra} = \sum_{i=1}^{n} w_i E_{intra}(i)$$

while E_{inter} is the sum of all nonbonded, *inter*molecular interactions between the molecules of the RM and those of RM ∪ SM

$$E_{inter} = \sum_{i=1}^{n} \sum_{j=i+1}^{n+n_{pack}} w_{ij} E_{inter}(i,j) \qquad (w_{ij} = w_i w_j)$$

where n_{pack} is the number of molecules in the SM and, when the j molecule belongs to SM, w_j is the occupancy factor of its "generating" molecule. To eliminate the intermolecular contribution due to different disordered components at a single crystallographic site in RM, we set w_{ij} = 0 if the molecules i and j are two mutually excluding components of RM. Note that, at variance from what we have done in ref 1, here all summations run over molecules rather than atoms; however, this does not imply a whole topological description of the SM because the only molecular property of interest is the site occupancy factor. E_s directly refers to a local property of the whole RM and is the functional to be minimized to optimize the crystal structure. However, it is convenient to define also global properties for each molecule in the RM, namely its potential packing energy *PPE*(i) and the derived E_s*

$$PPE(i) = \sum_{j=1(j\neq i)}^{n+n_{pack}} w_j E_{inter}(i,j)$$

$$E_s^{\bullet} = \sum_{i=1}^{n} w_i [E_{intra}(i) + {}^1/_2 PPE(i)]$$

to be used to compare computed steric energies with the global

(9) Harada, J.; Ogawa, K.; Tomoda, S. *Acta Crystallogr.* **1997**, *B53*, 662−672.

(10) Allinger, N. L.; Yuh, Y. H.; Lii, J.-H. *J. Am. Chem. Soc.* **1989**, *111*, 8551−8566. Lii, J.-H.; Allinger, N. L. *J. Am. Chem. Soc.* **1989**, *111*, 8566−8575. Lii, J.-H.; Allinger, N. L. *J. Am. Chem. Soc.* **1989**, *111*, 8576−8582.

Table 1. Comparison between Experimental and Computed Geometrical Parameters for Compounds **1** and **2**[a]

compd	T (K)	C(7)−C(7′) (Å)			C(1)−C(7)−C(7′) (deg)			C(6)−C(1)−C(7)−C(7′) (deg)			ref
$\mathbf{1}_\alpha$	298	1.295	*1.303*		125.8	*127.4*		3.3	*1.0*		3
	298	1.288			126.2			3.2			4
	295	1.328	–		126.8	–		3.6	–		6[b]
		1.330			126.2			5.3			
	113	1.331	*1.330*		126.1	*125.9*		3.4	*0.5*		5
$\mathbf{1}_\beta$	298	1.318	*1.321*		126.7	*126.7*		5.0	*8.4*		3
	298	1.313			127.0			5.6			4
	295	1.326			126.4			5.3			6
	113	1.341	*1.341*		126.0	*125.6*		6.9	*9.0*		5
2[c]	298	1.283	*1.271*	*1.239*	128.3	*129.5*	*131.2*	11.7	*13.8*	*12.9*	8
	234	1.300	*1.283*	*1.253*	127.3	*128.6*	*130.1*	13.6	*15.3*	*14.8*	8
	175	1.310	*1.298*	*1.272*	127.0	*127.5*	*128.8*	15.4	*17.2*	*17.5*	8
	118	1.321	*1.318*	*1.300*	126.4	*126.2*	*126.8*	18.0	*19.7*	*21.2*	8

[a] Computed values are given in italics. [b] Since ref 6 gives distinct values for the two disordered components which were, however, restrained to be similar to those of $\mathbf{1}_\beta$, a comparison with our computed values is not possible. [c] For compound **2** the two computed values quoted refer to the optimized and the original cell, respectively.

Scheme 1

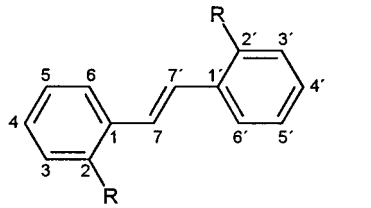

(**1**) R = H
(**2**) R = CH_3

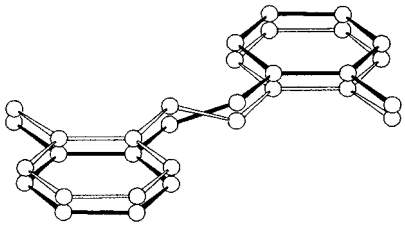

Figure 2. Superimposition of the two enantiomeric forms of (*E*)-2,2′-dimethylstilbene (**2**) according to Ogawa's dynamic model of disorder. The two molecules are related by a reflection plane nearly parallel to the aromatic rings, and differ in the orientation of the ethylene bond.

properties of the crystal. In particular, E_s* is related to the sublimation enthalpy *per* RM *cluster* by the following relation:

$$\Delta H_s = E_s^\bullet - \sum_{i=1}^{n} w_i E_{gas}(i)$$

where $E_{gas}(i)$ is the steric energy of the isolated molecule i in its gas phase conformation. When the n molecules in RM are equal (as in the case of **1**), the sublimation enthalpy *per mole of compound* can be obtained dividing by n, or more generally, by $\sum_{i=1}^{n} w_i$.

Results and Discussion

Origin of Disorder in 1. This problem has been previously tackled by Bernstein and Mirsky, who managed to include the degree of disorder at the α site in the evaluation of the lattice energy in their AAPP calculations;[11] their results were consistent with the preference for disorder at the α site only, and showed that its amount was limited to a maximum value of 20% at 298 K. The method outlined in the following, despite the similarities with that of Bernstein and Mirsky, allowing a *complete*

(11) Bernstein, J.; Mirsky, K. *Acta Crystallogr.* **1978**, *A34*, 161−165.

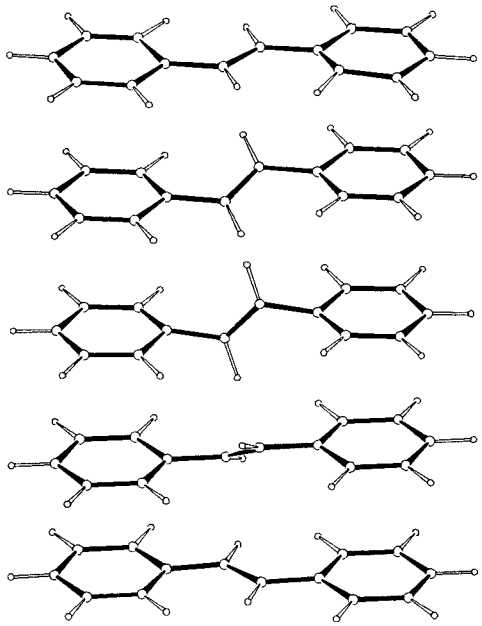

Figure 3. The mechanism of interconversion between $\mathbf{1}_\alpha$ and $\mathbf{1}_{\alpha'}$ at the α site of (*E*)-stilbene, according to Ogawa's pedal model. Wide vibrations of the C(6)−C(1)−C(7)−C(7′) and C(7)−C(7′)−C(1′)−C(6′) torsional angles lead to a transition state with the ethylene bond almost orthogonal to the plane of the aromatic rings, and eventually result in a 180° rotation of the ethylene bond about the C(1)···C(1′) axis.

optimization of the disordered crystal and, taking into account entropic contributions, should grant superior results. In detail, (i) four hypothetical, ordered crystals were generated from the four couples of independent molecules ($\mathbf{1}_\alpha$, $\mathbf{1}_\beta$), ($\mathbf{1}_{\alpha'}$, $\mathbf{1}_\beta$), ($\mathbf{1}_\alpha$, $\mathbf{1}_{\beta'}$), and ($\mathbf{1}_{\alpha'}$, $\mathbf{1}_{\beta'}$)—$\mathbf{1}_{\alpha'}$ and $\mathbf{1}_{\beta'}$ being related to $\mathbf{1}_\alpha$ and $\mathbf{1}_\beta$, respectively, by a 180° rotation about the C(1)···C(1′) direction; (ii) the ordered crystals were allowed to relax, finding relative sublimation enthalpies of 0, 0.16, 1.39, and 1.86 kcal mol^{-1}, respectively; this implies that the presence of disorder at the β site is considerably more costly than at the α one (in qualitative agreement with the fact that disorder is experimentally detected only at the α site) and allowed us to focus on the latter site only; (iii) relative sublimation enthalpies for the real, disordered crystal as a function of the fraction of disorder *at the* α *site* (p) were evaluated including the $\mathbf{1}_\alpha$, $\mathbf{1}_{\alpha'}$, and $\mathbf{1}_\beta$ molecules with site occupancy factors equals to $(1 - p)$, p, and 1, respectively, and employing the experimental cell parameters at rt (computations[12] have been done for p values from 0.0 to 1.0, in steps of 0.1);

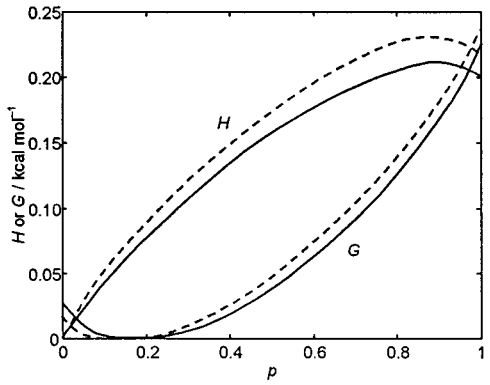

Figure 4. Dependence of the computed enthalpy (*H*) and free energy (*G*) from the amount of disorder at the α site in **1**. Solid and dashed lines have been obtained by interpolation of the data determined using the experimental (at rt) and the optimized cell parameters, respectively.

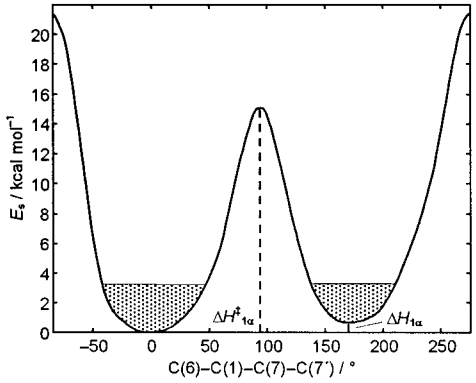

Figure 5. Energy profile along Ogawa's reaction path at the α site of (*E*)-stilbene (**1**$_\alpha$). The two minima differ by 0.7 kcal mol^{-1} ($\Delta H_{1\alpha}$), and are separated by an energy barrier of 15.1 kcal mol^{-1} ($\Delta H^{\ddagger}_{1\alpha}$), thus confirming the dynamic nature of the disorder. Being related by a 2-fold rotation of the ethylene bond about the C(1)···C(1′) axis, they prove the availability of Ogawa's mechanism for **1**$_\alpha$.

(iv) the configurational entropy *S* associated to disorder *at the* α *site only* (hence $n = {}^1/_2$) was calculated according to the usual Boltzmann formula

$$S = -nR[(1-p)\ln(1-p) + p\ln p]$$

The computed enthalpies at various degrees of disorder show that, from an enthalpic point of view, a perfectly ordered crystal ($p = 0.0$) is preferred (see Figure 4). However, since the configurational entropy has its maximum for $p = 0.50$, the Gibbs free energy function has its minimum for $p = 0.18$ (see Figure 4). This figure compares well with the experimental result obtained by Kroon et al. ($p = 0.13$)[6] and with that computed by Bernstein and Mirsky ($p < 0.20$), while the straight Boltzmann's statistics (applied to the relative energy of an **1**$_{\alpha'}$ molecule in the ordered (**1**$_\alpha$, **1**$_\beta$) crystal, $\Delta H_{1\alpha}$ in Figure 5) overestimates the disorder ($p = 0.25$). However, the above computations have been made using the rt experimental cell parameters which, referring to the *actual* disordered crystal, might bias the computational results. In particular, since we expect that the presence of some disorder determines a slight

(12) Computations have been done employing a localized bond model for the stilbene molecules (ITYPE 50 and 2, for the benzene and the ethylene carbon atoms, respectively) because the upgrade of the force-field parameters required by the delocalized model caused the optimization procedure to be unstable. However, we think that a localized model is adequate to describe the shape of the molecules in their minimum energy conformation, as needed to account for the static behaviour of the disordered model, since a very accurate description of torsional deformations is not necessary.

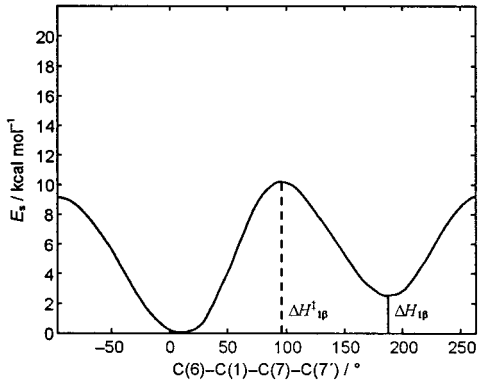

Figure 6. Energy profile along Ogawa's reaction path at the β site of (*E*)-stilbene (**1**$_\beta$). The two minima differ by 2.6 kcal mol^{-1} ($\Delta H_{1\beta}$), and are separated by an energy barrier of 9.7 kcal mol^{-1} ($\Delta H^{\ddagger}_{1\beta}$), thus suggesting, at variance from that proposed by Ogawa, the availability of the full rotation of the ethylene bond even at the β site.

increase of the cell volume, the potential packing energy of the ordered crystal could have been underestimated. Allowing cell optimization on minimizing the disordered crystals, we found that the volume does indeed increase on raising the amount of disorder and that the *G* minimum moves to a lower *p* (0.14), reaching an even better agreement with the experimental results (see Figure 4).

(*E*)-Stilbene Dynamics at the α Site. The energy profile for Ogawa's reaction path for **1**$_\alpha$ (see Figure 5) has been computed by applying a torsional driver (37 steps of 10° each) to the dihedral angles C(6)−C(1)−C(7)−C(7′) of the proper molecule (in the frozen crystal lattice). The presence of a center of symmetry has induced an opposite rotation of the C(6′)−C(1′)−C(7′)−C(7) angle. The overall deformation path resulted to be the "pedal" motion reported in Figure 2, i.e., a rotation of the C(7)−C(7′) bond about the C(1)···C(1′) axis, substantially not affecting the phenyl rings. Even by dropping the molecular center of symmetry, the isolated minima were centrosymmetric (and real stationary points on the whole potential energy hypersurface). The "real" path is not necessarily centrosymmetric, yet centrosymmetry was imposed to allow a comparison between the computational and the experimental results. The presence of two minima, related by a 2-fold rotation of the ethylene bond about the C(1)···C(1′) axis and with "similar" energies ($\Delta H_{1\alpha} = 0.7$ kcal mol^{-1}), is consistent with the observed disorder. Moreover, the presence of a "medium" energy barrier among them ($\Delta H^{\ddagger}_{\alpha} = 15.1$ kcal mol^{-1}) confirms the dynamic nature of this disorder, the feasibility of the pedal motion at rt and its quenching at 113 K (no disorder has been observed at that temperature).

(*E*)-Stilbene Dynamics at the β Site. It is noteworthy that the energy profile reported in Figure 6, computed as for **1**$_\alpha$, does not justify just a *limited* libration about the C(6)−C(1)−C(7)−C(7′) and C(7)−C(7′)−C(1′)−C(6′) torsional angles as proposed by Ogawa; furthermore, the computed $\Delta H^{\ddagger}_{1\beta}$ of 9.7 kcal mol^{-1} implies an even faster dynamics than that at site α. However, since $\Delta H_{1\beta}$ is much larger than $\Delta H_{1\alpha}$ (2.6 vs 0.7 kcal mol^{-1}), this motion does not result in any disorder and leaves only subtle traces in the diffraction results (i.e., the anomalous shortening of the C(7)−C(7′) bond length and its temperature dependence).

Quantitative Evaluation of Time Averaged Bonding Parameters in 1. The potential wells reported in Figures 5 and 6, associated with the torsional vibrations of the C(2,6)−C(1)−C(7)−C(7′)−C(1′)−C(2′,6′) moiety, are adequately wide to allow ample librations which, independently from the presence

of disorder, can be responsible for the apparent shrinking of the ethylene bond and, since the librational amplitude decreases with temperature, are also responsible for the anomalous lengthening of the ethylene bond on lowering the temperature. More importantly, the actual shape of these potential wells allows the computation of the time (thermal)-averaged values of the temperature-dependent geometrical parameters at the desired temperatures and to compare them with the corresponding experimental values (see Table 1). After the minima were localized, the shape of the reaction path in their vicinity (within a range of 3 kcal mol^{-1}) was determined in greater detail by a denser sampling (2° instead of 10°) of the reaction coordinate q. This allows a more realistic evaluation of the time (thermal)-averaged atomic locations $\langle \mathbf{x}_i \rangle$, which should be the X-ray diffraction observable, according to the following formulas:

$$w(q) = \frac{e^{-E(q)/RT}}{\int e^{-E(q)/RT} \mathrm{d}q}$$

$$\langle \mathbf{x}_i \rangle = \int w(q) \mathbf{x}_i(q) \mathrm{d}q$$

where the discreteness of the "vibrational" levels associated with the given potential well has been neglected. $w(q)$ are the Boltzmann's statistics weights and $\mathbf{x}_i(q)$ are the i atom coordinates at q (as estimated from our MMAAPP computations for each sampled point). We actually computed in this way the coordinates of C(1), C(6), C(7), and C(7′) deriving the related C(7)−C(7′) bond distance and C(1)−C(7)−C(7′) and C(6)−C(1)−C(7)−C(7′) angles therefrom. As long as $\mathbf{1}_\alpha$ is concerned, both Finder and Bernstein reported averaged geometrical parameters (they did not separate the two disordered individuals), whereas Boustra gave distinct values for $\mathbf{1}_\alpha$ and $\mathbf{1}_{\alpha'}$ which were, however, restrained to be similar to those of $\mathbf{1}_\beta$. Accordingly, even if we could carry out our computations within the individual $\mathbf{1}_\alpha$ or $\mathbf{1}_{\alpha'}$ potential wells, to compare our results with those of Finder and Bernstein, we computed the averages by considering in the integration both basins (which are shaded in Figure 5). From a qualitative point of view, the agreement is fairly good since, on decreasing the temperature, the two sets of parameters show the same trend. The agreement is good even from a quantitative point of view for all of the bonding interactions but for the C(6)−C(1)−C(7)−C(7′) and C(2)−C(1)−C(7)−C(7′) torsions. As for $\mathbf{1}_\beta$, again, from a qualitative point of view, the agreement is good. Quantitatively, the major discrepancy is once more found for the above torsions. Indeed, the averaged coordinates differ from the experimental ones within 0.01−0.05 Å, the C(2), C(2′), C(6), and C(6′) atomic positions being the more affected.

(*E*)-2,2′-Dimethylstilbene Dynamics. The energy profile for the pedal motion of **2**, determined as for $\mathbf{1}_\alpha$, is reported in Figure 7, where the solid line refers to the computations made with the experimental cell parameters, and the dashed line refers to those made with the optimized cell parameters (see Methodology). The two profiles are similar, definitely more complex than those for $\mathbf{1}_\alpha$ and $\mathbf{1}_\beta$, and since the highest barrier does not exceed 10 kcal mol^{-1}, the full pedal motion is allowed no matter which cell parameters are used in the simulation. Thus, as for the dynamics at site β, our computations suggest that Ogawa managed to recognize the nature of the observed phenomena but, lacking the proper tool for a quantitative evaluation of his proposal, failed to assess the actual amplitude of the libration. As for the shape of the potential well (see inset in Figure 7), the two profiles do convey different information. According to the solid profile, the presence of two minima (with ΔH_2 and $\Delta H^{\ddagger}_2$ of 0.6 and 0.06 kcal mol^{-1}, respectively, related by a mirror plane almost parallel to the aromatic rings) supports the disordered model proposed by Ogawa, who computed a ΔH_2 of 0.6 kcal mol^{-1} from the temperature dependence of the molecular site occupancy factors.[9] On the contrary, the dashed profile lacks the two mirror-related minima but presents a flat, asymmetric potential well, characterized by an inflection just where the other profile has the mirror-related minimum. These differences obviously persist also after the denser sampling of the reaction paths needed for the estimate of the time-averaged geometrical parameters and result in slightly different estimated values. In particular, the dashed path, even if lacking the two minima, affords a better match between experimental and theoretical trends (see Table 1). Quantitatively, the overall differences are well within the "expected" uncertainties of our computations; however, from a qualitative point of view, it may be thought that the two profiles convey different information about the eventual presence of disorder. The latter seems to be supported by the two minima present along the solid profile, while the dashed one should allow only large librational motion to be invoked. Yet, the barrier between the two minima is so small that their interconversion is very rapid, resulting in the very same ample libration permitted by the flat well of the dashed profile. Thus, according to both profiles, the molecule is affected by a very ample, fast librational motion, responsible both for the detected geometrical anomalies and for the uncertainties in individuating the supposed disorder. Indeed, a substantial interconvertion barrier like that separating $\mathbf{1}_\alpha$ from $\mathbf{1}_{\alpha'}$ allows more conclusive considerations about the presence of disorder. Actually, the difficulty in treating **2** emerges even in the work of Ogawa, where the site occupation factors resulting from the refinement of the structure at 298 and 118 K do not compare at all, both from a quantitative and from a qualitative point of view, with those evaluated on the basis of the disorder model. At this point we have also attempted to theoretically evaluate the amount of disorder, proceeding as in the case of **1**. Unfortunately, our results poorly agree with those computed by Ogawa (0.15 vs 0.35), even if cell optimization in the presence of the "experimental" amount of disorder (at 298 K)

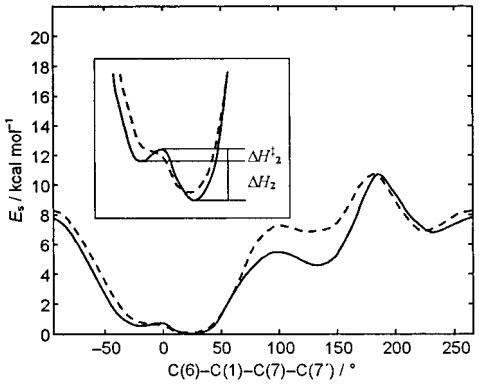

Figure 7. Energy profile along Ogawa's reaction path for (*E*)-2,2′-dimethylstilbene (**2**) computed using the experimental (—) and the optimized (- - -) cell parameters. Quantitatively, the overall differences are well within the expected uncertainties of our computations; however, from a qualitative point of view, it may be thought that the two profiles convey different information about the eventual presence of disorder. Yet, the barrier between the two minima in the solid profile is so small and their interconversion so rapid, that the overall motion is the very same ample libration permitted by the flat well of the dashed profile. Moreover, in both cases, the highest energy barrier does not exceed 10 kcal mol^{-1}, thus suggesting, at variance from that proposed by Ogawa, the availability of the full rotation of the ethylene bond.

affords cell parameters and volume in fair agreement with the experimental ones.

Conclusions

A dynamic process can be inferred by diffraction methods only if it leaves a track in the atomic displacement parameters (ADPs) and/or gives rise to some disorder or to some anomaly in the bonding parameters. However, since a diffraction experiment maps (according to Boltzmann's statistics) only the bottom of the local minima of potential energy profile many possible sources of misunderstanding are present. Indeed, as previously shown for the solid-state dynamics of $Fe_3(CO)_{12}$,[13] the presence of a soft vibrational mode (determining the ADPs shape) cannot exclude the occurrence of a more energetic, but still allowed, process along a different reaction path (not leaving tracks on the ADPs). Analogously, when Boltzmann's statistics assigns a negligible population to a reaction "intermediate", the failure to observe it cannot be used as an argument about the occurrence, or the amplitude of the dynamic process under scrutiny. Diffraction studies at different temperatures allow ascertaining the dynamic nature of temperature-dependent features, but still little can be said about the details of the observed dynamics. However, when variable temperature studies are coupled to molecular mechanics computations within the crystal lattice, a better modeling and hence a deeper insight, of the observed dynamics is possible. Here, we have shown that MMAAPP computations on a class of *flexible* (*E*)-stilbenes, offering a detailed description of the molecular solid-state trajectories (and of the involved energy changes), not only allow the confirmation the availability of the pedal motion but also lead to a *quantitative* evaluation of the anomalous temperature dependence of the ethylene bond parameters in these compounds.

Summarizing, our computations (i) afford a theoretical estimate, better than that of Bernstein and Mirsky,[11] of the disorder experimentally observed in **1**, (ii) confirm the substantial features of Ogawa's interpretation of the anomalous solid-state behavior of (*E*)-stilbenes, (iii) suggest that, at RT, the pedal motion is fully operative in all the situations here considered (**1**$_\alpha$, **1**$_\beta$, **2**), and (iv) allow a *quantitative* estimate of the anomalous temperature dependence of the ethylene bonding parameters in these compounds. (*E*)-Azobenzenes have solid-state structures and features very similar to those of (*E*)-stilbenes, and since we are inclined to believe that results similar to those obtained for (*E*)-stilbenes will emerge for (*E*)-azobenzenes as well, we are planning to extend our computational approach to that system.

Acknowledgment. The authors are indebted to N. Masciocchi for his careful reading of the manuscript. This work was supported by MURST (40%). S.G. thanks Montell for a research grant.

JA9842417

(13) Sironi, A. *Inorg. Chem.* **1996**, *35*, 1725−1728.